

# Thin films of gallium oxide obtained by spray-pyrolysis: method and properties

D.I. Panov<sup>1</sup>, X. Zhang<sup>1</sup>, V.A. Spiridonov<sup>1</sup>✉, L.V. Azina<sup>1</sup>, R.K. Nuryev<sup>1</sup>, N.D. Prasolov<sup>1</sup>,  
L.A. Sokura<sup>2</sup>, D.A. Bauman<sup>1</sup>, V.E. Bougrov<sup>1</sup>, A.E. Romanov<sup>1</sup>

<sup>1</sup>ITMO University, 49, Kronverkskiy Pr., St. Petersburg, Russia

<sup>2</sup>Ioffe Institute, 26, Polytekhnicheskaya St., St. Petersburg, 194021, Russia

✉ vladspiridonov@itmo.ru

**Abstract.** In this article, we report on fabricating thin solid films of gallium oxide by the spray-pyrolysis method. This method allows obtaining uniform thin films more easily compared with other sol-gel methods like spin-coating or dip-coating. In the experiment, sol concentrations were experimentally selected for further deposition on substrates. Morphology and chemical composition of the deposited films were studied by Scanning Electron Microscopy and Energy-Dispersive X-ray spectroscopy, respectively. The structural properties of the films were analyzed by X-ray diffraction method. The band gap of the Ga<sub>2</sub>O<sub>3</sub> films was estimated by analyzing the optical transmission spectra and was 4.87 eV. The quality and homogeneity of the obtained coatings are evaluated.

**Keywords:** Keywords: sol-gel, spray-pyrolysis, thin film, gallium oxide, ultrawide bandgap semiconductor

**Acknowledgements.** *The authors are grateful to Dr. A.M. Smirnov for valuable discussions. This study was done as part of the research program of the scientific school "Theory and practice of advanced materials and devices of optoelectronics and electronics" (scientific school 5082.2022.4)*

**Citation:** Panov DI, Zhang X, Spiridonov VA, Azina LV, Nuryev RK et al. Thin films of gallium oxide obtained by spray-pyrolysis: method and properties. *Materials Physics and Mechanics*. 2022;50(1): 107-117. DOI: 10.18149/MPM.5012022\_8.

## 1. Introduction

As a typical representative of the third-generation semiconductor materials,  $\beta$ -Ga<sub>2</sub>O<sub>3</sub> has attracted much attention because of its wide band gap (~4.8 eV), high breakdown electric field (> 8 MV/cm), and relatively high electron mobility (~150 cm<sup>2</sup>/Vs) [1-4]. This material has not only excellent optoelectronic properties but also good thermal and chemical stability. Therefore,  $\beta$ -Ga<sub>2</sub>O<sub>3</sub> becomes a candidate material for high-frequency high-power devices, photodetectors, solar cells, and sensors [2,5,6]. For example, it is reported that there is a MOSFET based on Ga<sub>2</sub>O<sub>3</sub> with a breakdown voltage above 1000V [7]. The value of  $\beta$ -Ga<sub>2</sub>O<sub>3</sub> bandgap corresponds to the solar-blind ultraviolet region, which makes up for the shortcomings of GaN and ZnO due to the performance degradation caused by doping, which is one of the current international research hotspots [8].

High-quality  $\beta$ -Ga<sub>2</sub>O<sub>3</sub> films play a significant role in the development of optoelectronic semiconductor devices, and the quality of thin films appreciably depends on the preparation method and process parameters. There are several methods of preparing Ga<sub>2</sub>O<sub>3</sub> films: Radio Frequency Magnetron Sputtering (RFMS) [9,10], Metal Organic Chemical Vapor Deposition (MOCVD) [4,11], Molecular-beam epitaxy (MBE) [12,13], Pulsed Laser Deposition (PLD) [14], halide vapor phase epitaxy (HVPE) [15] and sol-gel processing [16-18]. Compared with other methods, the sol-gel method is widely used in the preparation of oxide films and perovskite materials [18-20] because of its simple equipment, easy operation, no vacuum environment, and relatively low price [21,22]. There are three commonly used approaches to sol-gel methods: dip-coating [23], spin-coating [16] and spray-coating (spray-pyrolysis) [24,25]. The solution is usually applied to prepare single-crystal epitaxial films without high temperatures [23,26]. But this method is only suitable for soluble materials or soluble precursors which can be crystallized at low temperatures. Several studies have shown that the spray-pyrolysis method with a post-annealing process provides a formation of the Ga<sub>2</sub>O<sub>3</sub> crystal films of good quality [27,28]. This method was used in our work to obtain gallium oxide thin films. It is easier to obtain uniform gallium oxide thin films by the spray-pyrolysis method compared with the spin-coating one.

## 2. Experimental setup and methodology

In this work, Ga<sub>2</sub>O<sub>3</sub> films were prepared on silica glass (SiO<sub>2</sub>) substrates by the spray-pyrolysis method. To obtain a solution for preparing gallium oxide film, the gallium nitrate [Ga(NO<sub>3</sub>)<sub>3</sub>\*8H<sub>2</sub>O] (99,9%) was dissolved in ethylene glycol [C<sub>2</sub>H<sub>6</sub>O<sub>2</sub>] (99.5%) with addition of monoethanolamine [C<sub>2</sub>H<sub>7</sub>NO] (99.5%) as a stabilizer. The solution was mixed at 60°C for 60 minutes. The concentration of gallium nitride varied from 0.125 to 0.5 mol/l. The molarity of gallium nitrate and ethylene glycol was 0.25 mol/l while the molar ratio of gallium nitrate and monoethanolamine was 3:1. Silica glass substrates were ultrasonically cleaned with isopropyl alcohol for 10 minutes.

The experimental setup for the preparation of Ga<sub>2</sub>O<sub>3</sub> thin films by spray-pyrolysis is schematically shown in Fig. 1.

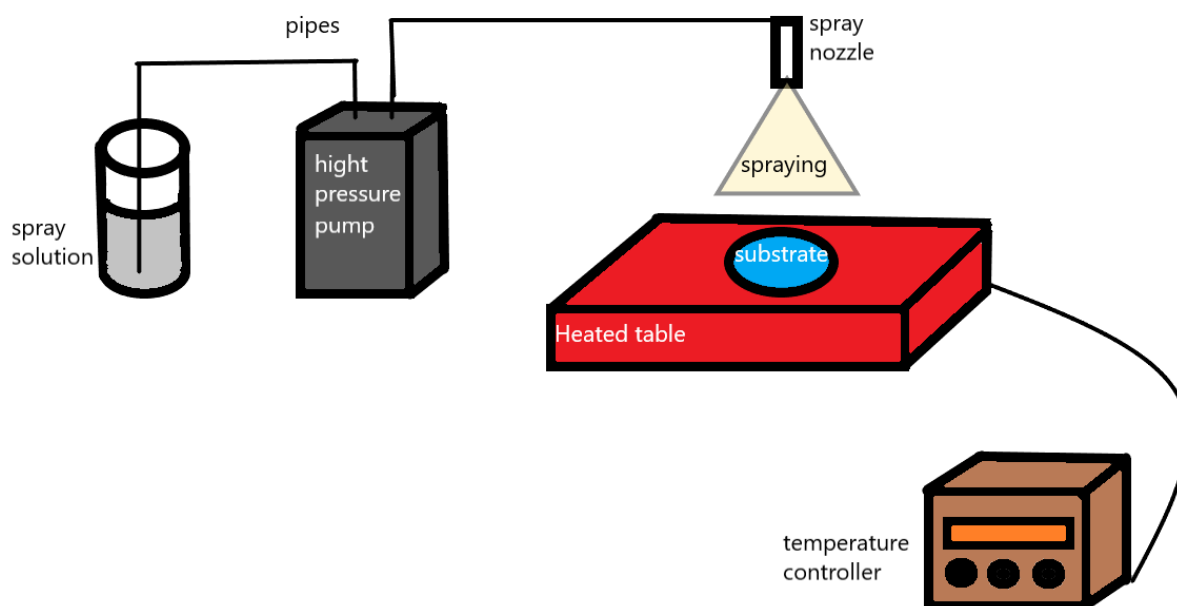


**Fig.1.** Schematics for spray-pyrolysis gallium oxide application unit

The solution was sprayed onto a substrate with the help of a high-pressure plunger pump and a spray nozzle with an outlet nozzle diameter of 0.1 mm. The substrate was located on a heated table connected to a temperature controller. The distance between the nozzle and the substrate was about 30 cm. Separate parts of the spraying system were connected by silicone pipes. The procedure of spraying is schematically shown in Fig. 2.

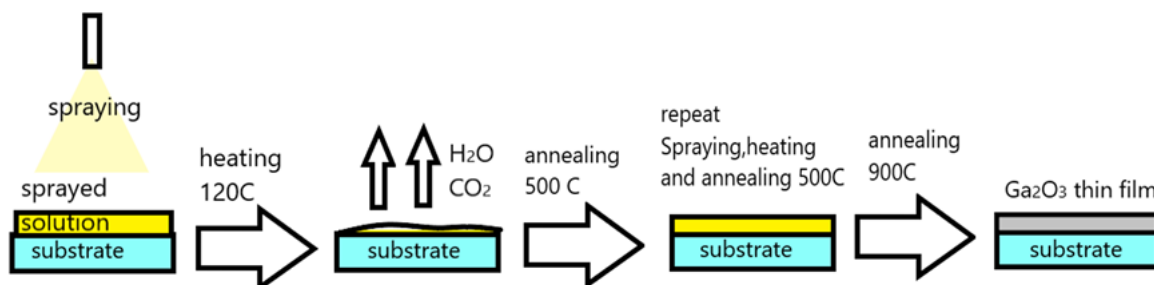
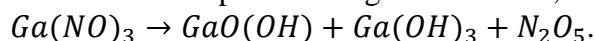
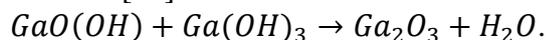


**Fig. 2.** Schematic representation of the spraying method with pre-annealing at 500°C

Every layer was deposited on the substrate at 120°C for 2 seconds. Then it was dried at 120°C for 120 seconds to get rid of water and carbon dioxide excesses. At this temperature there is a decomposition of gallium nitrate, which can be described by this reaction [29]:



The next step after drying was pre-annealing at 500°C for 5 minutes for each layer, to finally get rid of organic impurities. The process here can be described by the following reaction [29]:



After pre-annealing, the next layer was formed following the same procedure. This method, using pre-annealing at 500°C, was described by Zhu et. al. [17] as the optimal one, allowing to improve the quality of growing gallium oxide films. In our work, the process was repeated until 30 layers were deposited. The last step was the annealing of the sample at 900°C for 30 minutes for obtaining the beta phase of Ga<sub>2</sub>O<sub>3</sub>. The deposition and annealing processes were carried out in the air.

The morphology of gallium oxide films was characterized by AFM technique, using a Dimension 3100 microscope in dynamic contact mode. SEM images and EDX data of gallium oxide films were obtained by a TESCAN Mira 3 microscope with an Ultima MAX silicon drift detector. The XRD images were obtained using a Rigaku Ultima IV X-ray diffractometer (Japan). The radiation of a copper anode with  $\lambda$  (CuK $\alpha$ ) = 1.5418 Å was used. The radius of the goniometer was 285 mm. The X-ray was taken in the range of angles 2 $\theta$  from 15° to 70° in the geometry of the Bragg-Brentano survey. The measurements were carried out using a CuK $\beta$  filter. In the experiment, the voltage on the tube was 40 kV, and the current was 40 mA, the output power was 1.6 kW. The diffraction database International Center for Diffraction Data (ICDD) PDF-2 (2008) was used to interpret diffraction reflexes. The optical properties were studied in the range of 200-1000 nm by an optical spectrometer (AvasSpec-ThinFilm).

### 3. Results and discussion

The main goal of this work was to develop a method of forming a solid film of uniform thickness with a minimum number of defects (cracks, inclusions).

A series of experiments was carried out to figure out the optimal concentration of gallium nitrate, which ensures the formation of a solid film. On the one hand, higher

concentrations of metal ions led to larger numbers of nuclei during crystallization, resulting in smaller average grain sizes. On the other hand, spontaneous island crystallization and the formation of a highly inhomogeneous film are observed at too high concentrations of metal salts. An example of multiple island formations is clearly seen in Fig. 3. In this series of experiments, the concentration of gallium nitride varied from 0.125 to 0.5 mol/l. As a result, it was found that the optimal concentration was 0.25 mol/l.

The results of the studies presented below refer to the samples grown by spray pyrolysis with pre-annealing at 500°C and at the optimal concentration of gallium nitrate.

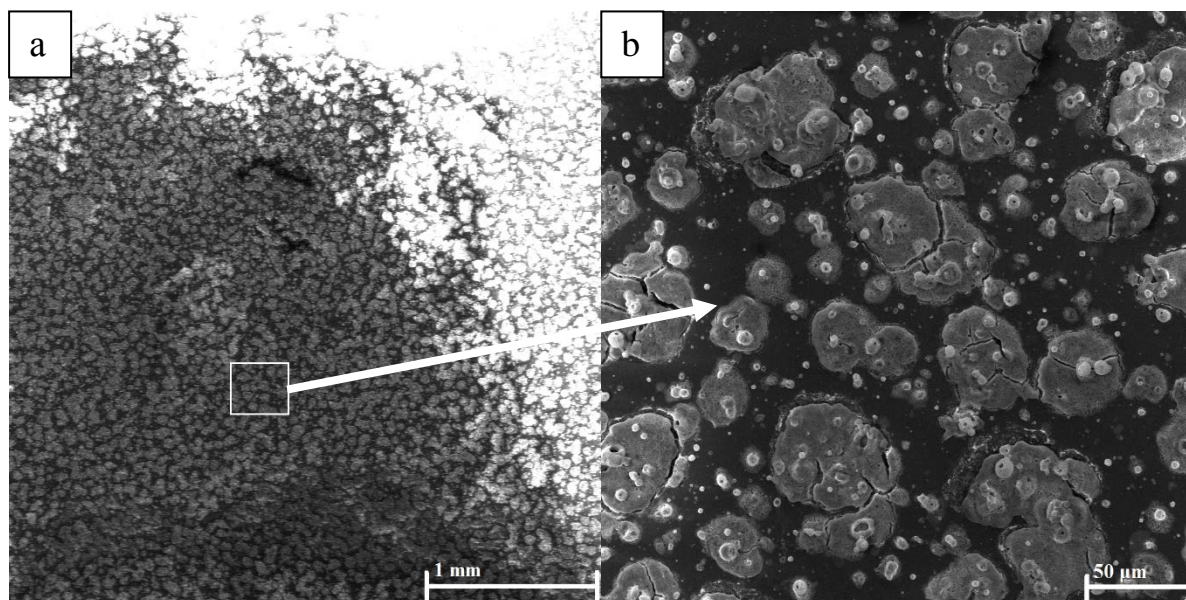


**Fig. 3.** Top-view SEM images gallium oxide film under varying magnification sample with 0.5 mol/l of gallium nitrate: a) scale 1 mm, b) scale 50 μm

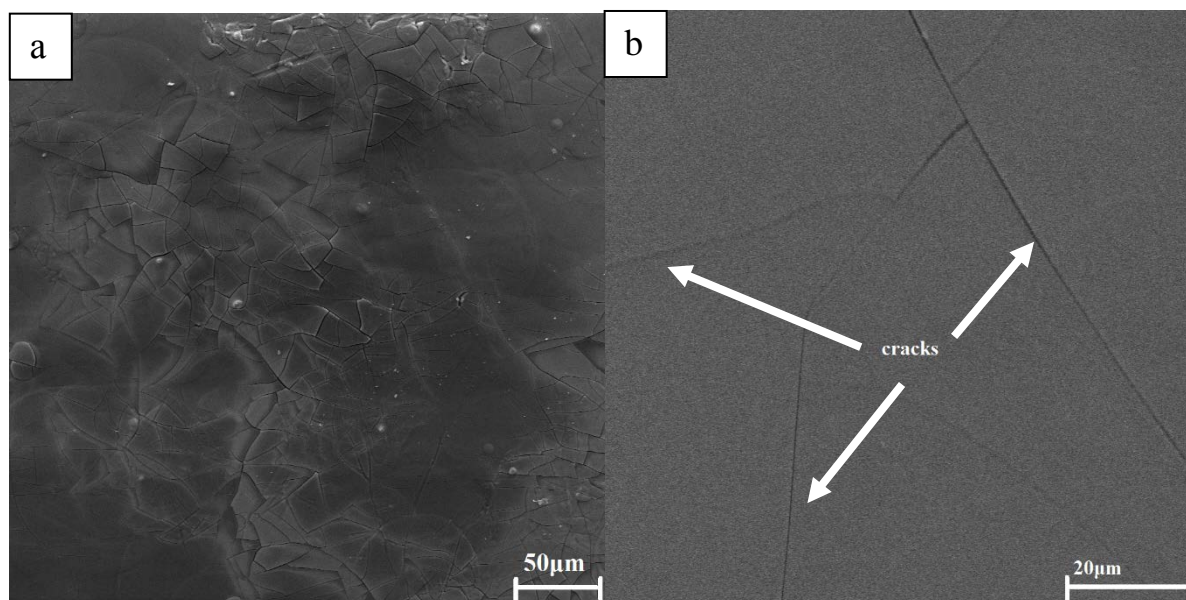
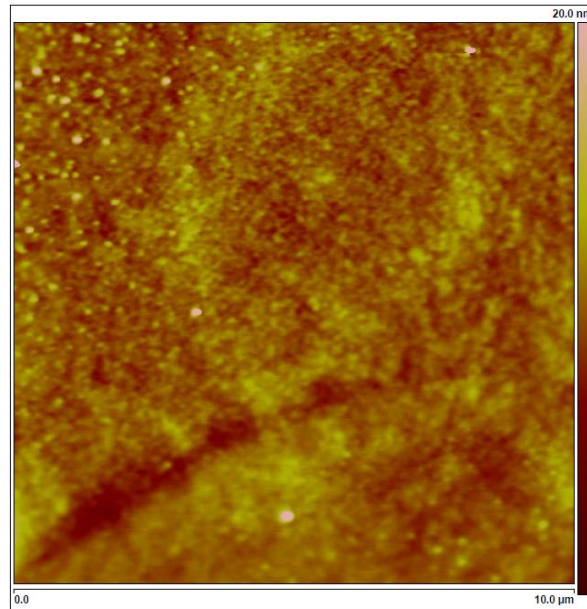


**Fig. 4.** Top view SEM images of the films with (0.25 mol/l) concentration of gallium nitrate: a) before heat treatment at 900°C, b) after heat treatment at 900°C

Figure 4 shows the surface morphology of the gallium oxide film before and after heat treatment at 900°C. As can be seen from the figure there are cracks on the film, which may be due to the different thermal expansion coefficients of the film (for  $\text{Ga}_2\text{O}_3 - 1.8 \times 10^{-6} \text{ K}^{-1}$  for

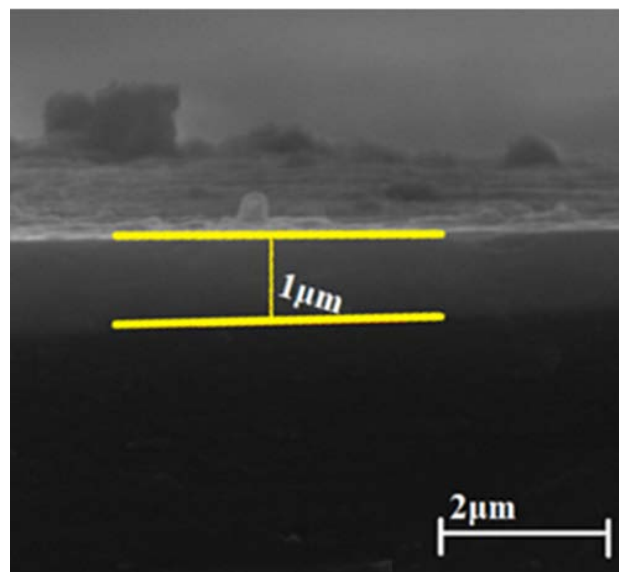
the  $a$  axis and  $4.2 \times 10^{-6} \text{ K}^{-1}$  for the  $b$  and  $c$  axes) [30] and the substrate (for fused silica is  $0.4 \times 10^{-6} \text{ K}^{-1}$ ) [31].

Figure 5 shows the AFM surface images of the same film. As can be seen from the surface scanning data, this  $\text{Ga}_2\text{O}_3$  film has average roughness  $R_a=0,954 \text{ nm}$  and square roughness  $R_q=1.21 \text{ nm}$  for a space of  $10 \mu\text{m} \times 10 \mu\text{m}$ .



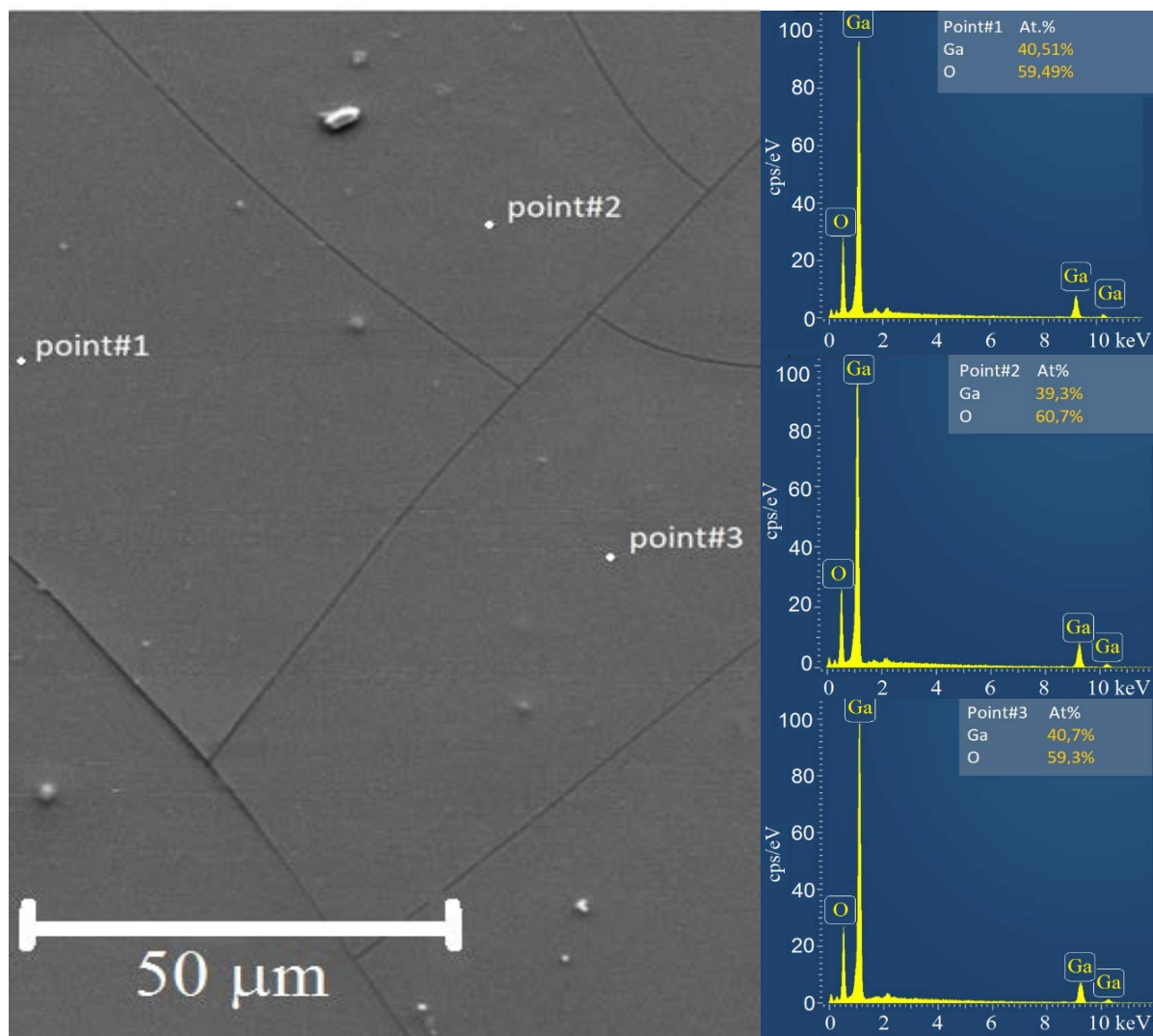
**Fig. 5.** AFM images ( $10 \mu\text{m} \times 10 \mu\text{m}$ ) of  $\beta\text{-Ga}_2\text{O}_3$  thin films annealed at  $900^\circ\text{C}$  ( $R_a=0.954 \text{ nm}$ ,  $R_q=1.21 \text{ nm}$ )

Figure 6 shows a cross-sectional SEM image of the substrate with a gallium oxide film deposited on it after a  $900^\circ\text{C}$  heat treatment. The film thickness at the middle area was about  $1 \mu\text{m}$ . A study across the entire width of the sample showed that the film thickness decreased near the edges to  $0.75 \mu\text{m}$ . This is most likely due to the conic shape of the spraying.



**Fig. 6.** The side view SEM image of the film: sample with optimal ( $0.25 \text{ mol/l}$ ) concentration of gallium citrate, the thickness of  $1 \mu\text{m}$

The chemical composition of obtained films was determined by the EDX (Energy Dispersive X-Ray Spectroscopy) method at several points and by EDX mapping over the film area. The results are shown in Fig. 7 and Fig. 8, respectively. The films have the correct stoichiometric composition  $\text{Ga}/\text{O} = 40/60$  distributed evenly over the entire area. The difference in composition values is less than 1.5% while the nominal accuracy of the method is about 0.5%.



**Fig. 7.** Results of film composition measurements by the EDX method. Left part of the figure: a top view SEM image of measurement area. Three points of measurements are marked. Right part of the figure: EDX spectra

X-ray diffraction (XRD) spectrum is shown in Fig. 9. In terms of position and integral intensity, the X-ray diffraction peaks of obtained thin films of  $\text{Ga}_2\text{O}_3$  by spray-pyrolysis method, after annealing at  $900^\circ\text{C}$ , correspond to  $\beta\text{-Ga}_2\text{O}_3$  ICDD data (PDF 00-041-1103). The size of crystallites reached 10 nm. The size of the crystallites was found by the Scherrer equation:

$$l = K * \lambda / (\beta * \text{Cos } \theta), \quad (1)$$

where  $\lambda$  is the X-ray wavelength in nanometer (nm),  $\beta$  is the peak width at half maximum height (rad), and  $K$  is a constant related to crystallite shape (0.94).

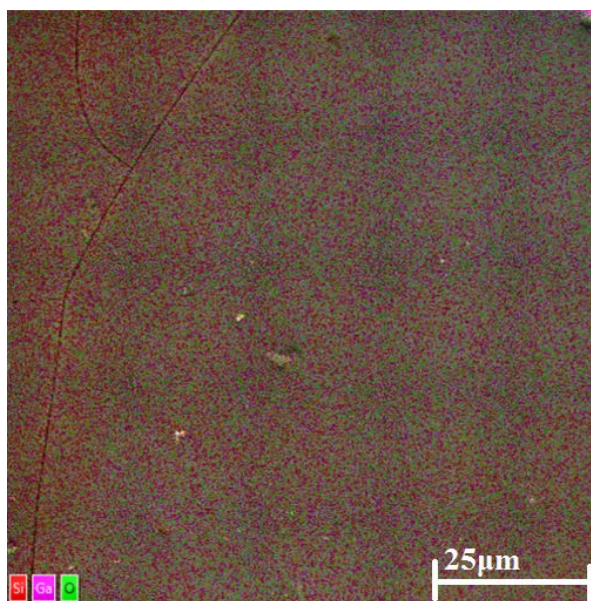


**Fig. 8.** Results of film composition study by the EDX mapping method: view SEM image of measurements area. The distribution of Ga, Si, and O elements on the resulting sample is shown in different colors

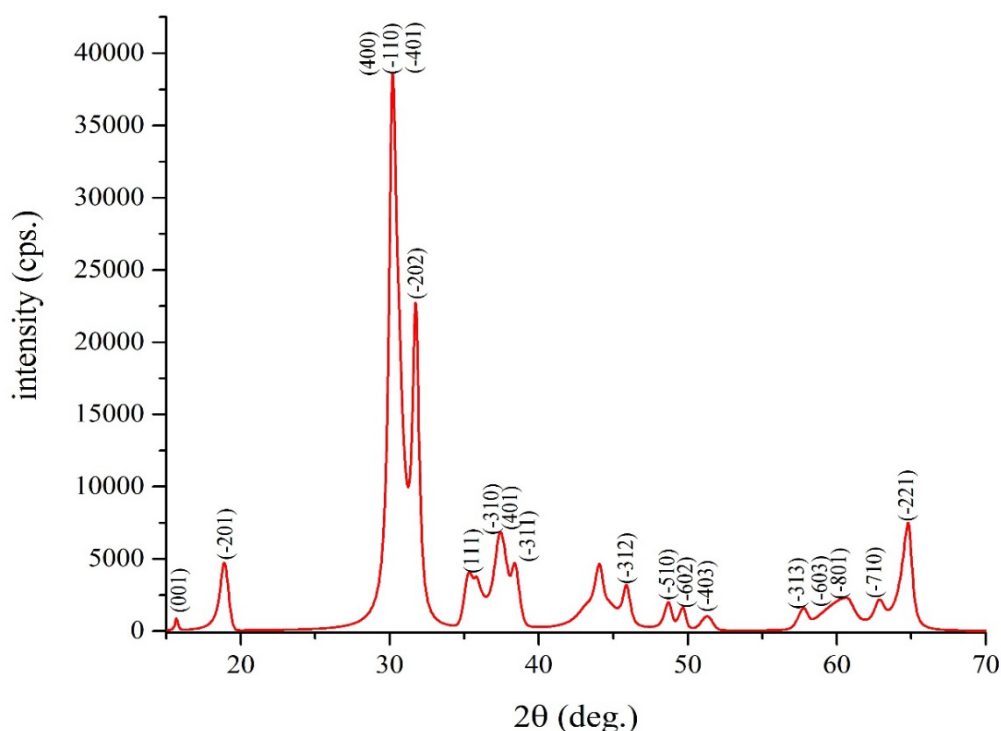


**Fig. 9.** X-ray diffraction (XRD) pattern of obtained thin films of  $\text{Ga}_2\text{O}_3$  by spray-pyrolysis method, after annealing at  $900^\circ\text{C}$ , indexed in comparison to PDF 00-041-1103

The calculated lattice constants for a thin film of gallium oxide after heat treatment  $900^\circ\text{C}$  were  $a = 12.1966(\text{\AA})$ ,  $b = 3.0313(\text{\AA})$ ,  $c = 5.7934(\text{\AA})$  ( $\alpha = 90.0^\circ$ ,  $\beta = 103.82^\circ$ ,  $\gamma = 90.0^\circ$ ), which corresponds to  $\beta\text{-Ga}_2\text{O}_3$  [32].

Transmission spectra of samples and bandgap estimation are shown in Fig. 10. The samples have transmission in the near-ultraviolet (N-UV), visible, and near-infrared (NIR) regions of the spectrum (300-1000 nm), and have an absorption band in the range of 200-250 nm. Also, it should be noted that after heat treatment of samples at  $900^\circ\text{C}$ , the

samples have a more intensive absorption in the range of 200-250 nm and more intensive transmission in the range of 300-1000 nm. This can be explained by the transition of the film to a crystalline state and the formation of beta phase of gallium oxide. Based on the optical absorption data, the bandgap value was estimated for the  $\beta$ -Ga<sub>2</sub>O<sub>3</sub> film after heat treatment at 900°C by analyzing transmission spectra [32,33]. The estimation gives a value of about 4.87 eV for the band gap which corresponds with the value of  $\beta$ -Ga<sub>2</sub>O<sub>3</sub> bandgap in previous works. [8,33,34].

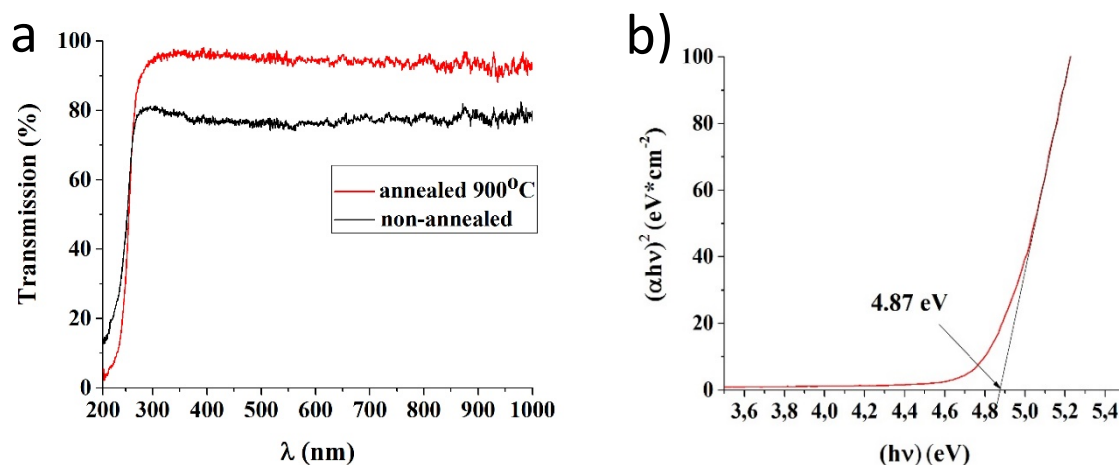


**Fig.10.** (a) Optical transmission spectra for annealed and non-annealed samples and substrate and (b) bandgap estimation for annealed at 900°C Ga<sub>2</sub>O<sub>3</sub> film

#### 4. Conclusions

A modification of the spray-pyrolysis method for the formation of gallium oxide solid films was proposed. The optimal value of the concentration of gallium nitrate was found to be 0.25, which ensures the formation of a solid film. At the optimal concentration of gallium nitrate, the preliminary annealing at 500°C was added to the method after deposition and drying of each layer. It was found that the proposed method ensures the formation of thin (up to 1 μm) solid films of gallium oxide on silica glass substrates. Analysis of the chemical composition by the EDS method showed the correct stoichiometric composition (Ga:O = 2:3) over the entire area of the film. It was proved by X-ray diffraction that the entire film consists of the beta phase of gallium oxide. An analysis of the transmission spectra made it possible to estimate the band gap of the material, which was 4.87 eV.

#### References

1. Pearton SJ, Yang J, Cary PH, Ren F, Kim J, Tadjer MJ, Mastro MA. A review of Ga<sub>2</sub>O<sub>3</sub> materials, processing, and devices. *Applied Physics Reviews*. 2018;5: 011301.
2. Stepanov SI, Nikolaev VI, Bougrov VE, Romanov AE. Gallium oxide: properties and applications – a review. *Reviews On Advanced Materials Science*. 2016;44: 63-86.
3. Galazka Z.  $\beta$ -Ga<sub>2</sub>O<sub>3</sub> for wide-bandgap electronics and optoelectronics. *Semiconductor Science and Technology*. 2018;33: 113001.
4. Bauman DA, Borodkin AI, Petrenko AA, Panov DI, Kremleva AV, Spiridonov VA, Zakgeim DA, Silnikov MV, Odnoblyudov MA, Romanov AE, Bougrov VE. On improving the radiation resistance of gallium oxide for space applications. *Acta Astronautica*. 2021;180: 125-129.
5. Yu M, Lv C, Yu J, Shen Y, Yuan L, Hu J, Zhang S, Cheng H, Zhang Y, Jia R. High-performance photodetector based on sol-gel epitaxially grown  $\alpha/\beta$ -Ga<sub>2</sub>O<sub>3</sub> thin films. *Materials Today Communications*. 2020;25: 101532.

6. Wenckstern H. Group-III Sesquioxides: Growth, Physical Properties and Devices. *Advanced Electronic Materials*. 2017;3: 1600350.
7. Hu Z, Nomoto K, Li W, Zhang Z, Tanen N, Thieu QT, Sasaki K, Kuramata A, Nakamura T, Jena D, Xing HG. Breakdown mechanism in 1 kA/cm<sup>2</sup> and 960 V E-mode  $\beta$ -Ga<sub>2</sub>O<sub>3</sub> vertical transistors. *Applied Physics Letters*. 2018;113: 122103.
8. Galazka Z, Irmscher K, Uecker R, Bertram R, Pietsch M, Kwasniewski A, Naumann M, Schulz T, Schewski R, Klimm D, Bickermann M. On the bulk  $\beta$ -Ga<sub>2</sub>O<sub>3</sub> single crystals grown by the Czochralski method. *Journal of Crystal Growth*. 2014;404: 184-191.
9. Zhang X, Jiang D, Zhao M, Zhang H, Li M, Xing M, Han J, Romanov AE. The effect of annealing temperature on Ga<sub>2</sub>O<sub>3</sub> film properties. *Journal of Physics: Conference Series*. 2021;1965: 012066.
10. Yin-nü. Preparation and Properties of Zn-doped  $\beta$ -Ga<sub>2</sub>O<sub>3</sub> Films. *Acta Photonica Sinica*. 2012;41: 1242-1246.
11. Du X, Mi W, Luan C, Li Z, Xia C, Ma J. Characterization of homoepitaxial  $\beta$ -Ga<sub>2</sub>O<sub>3</sub> films prepared by metal-organic chemical vapor deposition. *Journal of Crystal Growth*. 2014;404: 75-79.
12. Hassa A, Wouters C, Kneiß M, Splith D, Sturm C, Wenckstern H von, Albrecht M, Lorenz M, Grundmann M. Control of phase formation of (Al<sub>x</sub>Ga<sub>1-x</sub>)<sub>2</sub>O<sub>3</sub> thin films on c-plane Al<sub>2</sub>O<sub>3</sub>. *Journal of Physics D: Applied Physics*. 2020;53: 485105.
13. Kaun SW, Wu F, Speck JS.  $\beta$ -(Al<sub>x</sub>Ga<sub>1-x</sub>)<sub>2</sub>O<sub>3</sub>/Ga<sub>2</sub>O<sub>3</sub> (010) heterostructures grown on  $\beta$ -Ga<sub>2</sub>O<sub>3</sub> (010) substrates by plasma-assisted molecular beam epitaxy. *Journal of Vacuum Science & Technology A*. 2015;33: 041508.
14. Goyal A, Yadav BS, Thakur OP, Kapoor AK, Muralidharan R. Effect of annealing on  $\beta$ -Ga<sub>2</sub>O<sub>3</sub> film grown by pulsed laser deposition technique. *Journal of Alloys and Compounds*. 2014;583: 214-219.
15. Kremleva AV, Sharofidinov ShSh, Smirnov AM, Podlesnov E, Dorogov MV, Odnoblyudov MA, Bougrov VE, Romanov AE. Growth of thick gallium oxide on the various substrates by halide vapor phase epitaxy. *Materials Physics and Mechanics*. 2020;44(2): 164-171
16. Zhu Y, Xiu X, Cheng F, Li Y, Xie Z, Tao T, Chen P, Liu B, Zhang R, Zheng Y-D. Growth and nitridation of  $\beta$ -Ga<sub>2</sub>O<sub>3</sub> thin films by Sol-Gel spin-coating epitaxy with post-annealing process. *Journal of Sol-Gel Science and Technology*. 2021;100: 183-191.
17. Cheah LB, Osman RAM, Poopalan P. Ga<sub>2</sub>O<sub>3</sub> thin films by sol-gel method its optical properties. *AIP Conference Proceedings*. 2020;2203: 020028.
18. Yu L-Y, Shen H-M, Xu Z-L. PVDF-TiO<sub>2</sub> composite hollow fiber ultrafiltration membranes prepared by TiO<sub>2</sub> sol-gel method and blending method. *Journal of Applied Polymer Science*. 2009;113: 1763-1772.
19. Salles P, Caño I, Guzman R, Dore C, Mihi A, Zhou W, Coll M. Facile Chemical Route to Prepare Water Soluble Epitaxial Sr<sub>3</sub>Al<sub>2</sub>O<sub>6</sub> Sacrificial Layers for Free-Standing Oxides. *Advanced Materials Interfaces*. 2021;8: 2001643.
20. Brunckova H, Medvecký L, Briancin J, Durisin J, Mudra E, Sebek M, Kovalčíková A, Sopčák T. Perovskite lanthanum niobate and tantalate thin films prepared by sol-gel method. *Materials Letters*. 2016;165: 239-242.
21. Corriu RJP, Leclercq D. Recent Developments of Molecular Chemistry for Sol-Gel Processes. *Angewandte Chemie International Edition in English*. 1996;35: 1420-1436.
22. Andronic L, Perniu D, Duta A. Synergistic effect between TiO<sub>2</sub> sol-gel and Degussa P25 in dye photodegradation. *Journal of Sol-Gel Science and Technology*. 2013;66: 472-480.
23. Kelso MV, Mahenderkar NK, Chen Q, Tubbesing JZ, Switzer JA. Spin coating epitaxial films. *Science*. 2019;364: 166-169.

24. Kokubun Y, Miura K, Endo F, Nakagomi S. Sol-gel prepared  $\beta$ -Ga<sub>2</sub>O<sub>3</sub> thin films for ultraviolet photodetectors. *Applied Physics Letters*. 2007;90: 031912.
25. Shen H, Yin Y, Tian K, Baskaran K, Duan L, Zhao X, Tiwari A. Growth and characterization of  $\beta$ -Ga<sub>2</sub>O<sub>3</sub> thin films by sol-gel method for fast-response solar-blind ultraviolet photodetectors. *Journal of Alloys and Compounds*. 2018;766: 601-608.
26. Ohya Y, Okano J, Kasuya Y, Ban T. Fabrication of Ga<sub>2</sub>O<sub>3</sub> thin films by aqueous solution deposition. *Journal of the Ceramic Society of Japan*. 2009;117: 973-977.
27. Winkler N, Wibowo RA, Kautek W, Ligorio G, List-Kratochvil EJW, Dimopoulos T. Nanocrystalline Ga<sub>2</sub>O<sub>3</sub> films deposited by spray pyrolysis from water-based solutions on glass and TCO substrates. *Journal of Materials Chemistry C*. 2018;7: 69-77.
28. Kim H, Kim W. Optical properties of  $\beta$ -Ga<sub>2</sub>O<sub>3</sub> and  $\alpha$ -Ga<sub>2</sub>O<sub>3</sub>:Co thin films grown by spray pyrolysis. *Journal of Applied Physics*. 1987;62: 2000-2002.
29. Berbenni V, Milanese C, Bruni G, Marini A. Thermal decomposition of gallium nitrate hydrate Ga(NO<sub>3</sub>)<sub>3</sub>·xH<sub>2</sub>O. *Journal of Thermal Analysis and Calorimetry*. 2005; 82: 401-407.
30. Villora EG, Shimamura K, Ujiie T, Aoki K. Electrical conductivity and lattice expansion of  $\beta$ -Ga<sub>2</sub>O<sub>3</sub> below room temperature. *Applied Physics Letters*. 2008;92: 202118.
31. Oishi J, Kimura T. Thermal Expansion of Fused Quartz. *Metrologia*. 1969;5: 50-55.
32. Dohy D, Gavarrì JR. Oxyde  $\beta$ -Ga<sub>2</sub>O<sub>3</sub>: Champ de force, dilatation thermique, et rigidité anisotropes. *Journal of Solid State Chemistry*. 1983;49: 107-117.
33. Tauc J. Optical properties and electronic structure of amorphous Ge and Si. *Materials Research Bulletin*. 1968;3: 37-46.
34. Zakgeim D, Bauman D, Panov D, Spiridonov V, Kremleva A, Smirnov A, Odnoblyudov M, Romanov A, Bougrov V. Growing of bulk  $\beta$ -(Al<sub>x</sub>Ga<sub>1-x</sub>)<sub>2</sub>O<sub>3</sub> crystals from the melt by Czochralski method and investigation of their structural and optical properties. *Applied Physics Express*. 2022;15: 025501.

## THE AUTHORS

### **Panov D.I.**

e-mail: Dmitriipnv@gmail.com

ORCID: 0000-0001-8715-9505

### **Zhang X.**

e-mail: 314519083@qq.com

ORCID: 0000-0002-1275-1165

### **Spiridonov V.A.**

e-mail: vladspiridonov@itmo.ru

ORCID: 0000-0001-5751-8597

### **Azina L.V.**

e-mail: lvazina@itmo.ru

ORCID: 0000-0003-3502-1365

### **Nuryev R.K.**

e-mail: nuryev@itmo.ru

ORCID: 0000-0001-9427-1749

**Prasolov N. D.**

e-mail: ndprasolov@corp.ifmo.ru

ORCID: -

**Sokura L.A.**

e-mail: sokura@mail.ioffe.ru

ORCID: -

**Bauman D.A.**

e-mail: dabauman@itmo.ru

ORCID: 0000-0001-5751-8597

**Bougrov V.E.**

e-mail: Vladislav.bougrov@niuitmo.ru

ORCID: 0000-0001-5751-8597

**Romanov A.E.**

e-mail: alexey.romanov@niuitmo.ru

ORCID: 0000-0003-3738-408X